Plant Physiology and Biochemistry 137 (2019) 1–13

Contents lists available at ScienceDirect

Plant Physiology and Biochemistry

journal homepage: www.elsevier.com/locate/plaphy

Research article

Early stage metabolic events associated with the establishment of *Vitis vinifera – Plasmopara viticola* compatible interaction

Rui Nascimento[a,1], Marisa Maia[a,b,c,1], António E.N. Ferreira[b,c], Anabela B. Silva[a], Ana Ponces Freire[c], Carlos Cordeiro[b,c], Marta Sousa Silva[b,c,**,2], Andreia Figueiredo[a,*,2]

[a] Biosystems & Integrative Sciences Institute (BioISI), Science Faculty of Lisbon University, 1749-016, Lisboa, Portugal
[b] Laboratório de FTICR e Espectrometria de Massa Estrutural, Faculdade de Ciências da Universidade de Lisboa, Portugal
[c] Centro de Química e Bioquímica, Faculdade de Ciências da Universidade de Lisboa, Portugal

ARTICLE INFO

Keywords:
Metabolic regulation
Lipids
Carbohydrate metabolism
Downy mildew

ABSTRACT

Grapevine (*Vitis vinifera* L.) is the most widely cultivated and economically important fruit crop in the world, with 7.5 million of production area in 2017. The domesticated varieties of grapevine are highly susceptible to many fungal infections, of which downy mildew, caused by the biotrophic oomycete *Plasmopara viticola* (Berk. et Curt.) Berl. et de Toni is one of the most threatening. In *V. vinifera*, several studies have shown that a weak and transient activation of a defense mechanism occurs, but it is easily overcome by the pathogen leading to the establishment of a compatible interaction. Major transcript, protein and physiologic changes were shown to occur at later infection time-points, but comprehensive data on the first hours of interaction is scarce.

In the present work, we investigated the major physiologic and metabolic changes that occur in the first 24 h of interaction between *V. vinifera* cultivar Trincadeira and *P. viticola*. Our results show that there was a negative modulation of several metabolic classes associated to pathogen defense such as flavonoids or phenylpropanoids as well as an alteration of carbohydrate content after inoculation with the pathogen. We also found an accumulation of hydrogen peroxide and increase of lipid peroxidation but to a low extent, that seems to be insufficient to restrain pathogen growth during the initial biotrophic phase of the interaction.

1. Introduction

Grapevine (*Vitis vinifera* L.) has deep ties to human culture dated to more than 5000 years (McGovern et al., 1996). Being the most widely cultivated and economically important fruit crop in the world, this crop plays a key role in many countries economy, with a global market size of over 29 billion euros (Organization of Vine and Wine, 2017). However, most winegrowing grapevine cultivars are often affected by fungal pathogens causing severe harvest losses. One of these diseases, commonly known as downy mildew (DM), is caused by the obligate biotrophic oomycete *Plasmopara viticola* (Berk. et Curt.) Berl. et de Toni, unintentionally introduced into Europe in the late 19th century (Gessler et al., 2011). With adequate climate conditions, i.e. high humidity and moderate temperatures, *P. viticola* mature sporangia releases zoospores that are able to settle on the abaxial surface of leaves. These zoospores germinate and penetrate the stomatal cavity forming a substomatal vesicle, which in part gives rise to the primary hyphae and mycelium. The hyphae and mycelium invade the intercellular spaces differentiating specialized structures (haustoria) that penetrate parenchyma cell walls without breaking the plasma membrane, thus creating an intimate contact between the pathogen and the host. This biotrophic strategy is supposed to rely on a pathogen-driven manipulation of host cell metabolism and suppression of defense responses (Liu et al., 2015; Yin et al., 2017). The mycelium also develops to form sporangiophores emerging from the stoma releasing sporangia to the other grapevine tissues (leaves, twigs or grape clusters) and surrounding plants (Buonassisi et al., 2017; Gessler et al., 2011). As a result, *P. viticola* has devastating effects on unprotected crops, reducing grape quality and destroying up to 75% of production in a single season leading to massive economic losses (Armijo et al., 2016; Buonassisi et al., 2017;

* Corresponding author. Biosystems & Integrative Sciences Institute (BioISI), Faculdade de Ciências da Universidade de Lisboa, 1749-016, Lisboa, Portugal.
** Corresponding author. Laboratório de FTICR e Espectrometria de Massa Estrutural and Centro de Química e Bioquímica, Departamento de Química e Bioquímica, Faculdade de Ciências da Universidade de Lisboa, Portugal.
E-mail addresses: mfsilva@fc.ul.pt (M.S. Silva), aafigueiredo@fc.ul.pt (A. Figueiredo).
[1] These authors have contributed equally.
[2] These are both senior authors.

https://doi.org/10.1016/j.plaphy.2019.01.026
Received 16 October 2018; Received in revised form 17 January 2019; Accepted 18 January 2019
Available online 25 January 2019

Abbreviations

DFR	Dihydroflavonol Reductase
DM	Downy mildew
DNS	Dinitrosalicylic acid
EF1α	Elongation Factor 1-alpha
ESI	Electrospray ionization
F3′5′H	Flavonoid-3,5′-hydroxylase
FA	Fatty acyls
FatB	Palmitoyl-acyl carrier protein thioesterase
FLS	Flavonol Synthase/Flavanone 3-hydroxylase gene family
FTICR-MS	Fourier Transform Ion Cyclotron Resonance Mass Spectrometer
HMDB	Human Metabolome Database
hpi	Hours post inoculation
KEGG	Kyoto Encyclopedia of Genes and Genomes
LipA	Lipoyl Synthase
MDA	Malonaldehyde
PLS-DA	Partial least squares - discriminant analysis
PR	Pathogenesis-related
PVPP	Polyvinylpolypyrrolidone
qPCR	Quantitative real time Polymerase Chain Reaction
RFOs	Raffinose family of oligosaccharides
ROS	Reactive oxygen species
SAND	SAND family
TBA	Thiobarbituric acid
TPR7B	Tetratricopeptide repeat protein 7B
VIP	Variable Importance in Projection

Gessler et al., 2011; Kamoun et al., 2015; Madden et al., 2000).

Frequently the difference between a resistant and a susceptible plant is just a question of timing and amplitude of the adequate defense response (Figueiredo et al., 2012; Polesani et al., 2010). Despite the incompatible interaction being characterized to a greater extent, the knowledge on compatible interactions may provide information on the availability of defense mechanisms, but also aid in the development of new control strategies and possibly lead to the identification of pathogen and host factors needed for disease progression (Legay et al., 2011).

The infection process in susceptible genotypes is poorly characterized, in part because *P. viticola* is a strictly biotrophic parasite that can only grow on its natural host and not *in vitro*, which makes it difficult to study. The susceptibility of *Vitis vinifera* to downy mildew suggests that this species lacks a *P. viticola*-specific recognition system that enables the activation of a successful defense mechanism (Gaspero et al., 2007). To elucidate the *P. viticola* compatible interaction with grapevine, several omic-based studies have been published (Ali et al., 2012; Batovska et al., 2009; Becker et al., 2013; Chitarrini et al., 2017; Legay et al., 2011; Milli et al., 2012). Generally, grapevine-*P. viticola* compatible interaction is characterized by a global down-regulation of photosynthesis-related processes and inadequate up-regulation of genes encoding pathogenesis-related (PR) proteins, enzymes of phenylpropanoid pathways and regulators of response to stimuli (Legay et al., 2011; Ma et al., 2018; Perazzolli et al., 2012; Polesani et al., 2008; Su et al., 2018; Vannozzi et al., 2012). Gene expression analyses and proteomic studies also shown an accumulation of allergenic defense-related proteins (PR-2 and b-1,3-glucanases) (Rossin et al., 2015) and glycoproteins involved in the DM-induced deregulation of stomata during compatible interactions (Guillier et al., 2015) and the phosphorylation of photosynthesis and metabolism related proteins (Perazzolli et al., 2016). Grapevine-*P. viticola* metabolomic data is scarce, particularly on compatible interactions. We have previously used nuclear magnetic resonance (NMR) spectroscopy to characterize the main metabolic differences of compatible and incompatible interactions (Ali et al., 2012). We have shown that tolerant and susceptible cultivars not only possess distinct metabolic profile but also respond differently when confronted with biotic stress (Figueiredo et al., 2008; Ali et al., 2012), however our approach was not focused on the characterization of the compatible interaction.

We therefore carried out a deeper comparative metabolic analysis of grapevine leaves from the susceptible cultivar Trincadeira, at early time points following inoculation with *P. viticola*. We have followed an untargeted analysis based on Fourier Transform Ion Cyclotron Resonance Mass Spectrometry (FTICR-MS), together with biochemical and molecular approaches to identify key metabolic events underlying host susceptibility. Our data provides insight into the mechanisms underlying infection and colonization that leads to the establishment of a compatible interaction.

2. Materials and methods

2.1. Inoculation experiments

P. viticola inoculations were made in greenhouse grown *Vitis vinifera* cv Trincadeira plants, as previously described (Figueiredo et al., 2012). Briefly, a *P. viticola* population was collected from symptomatic leaves from greenhouse infected plants after an overnight incubation in a moist chamber at room temperature. Sporangia were carefully collected by brushing from de abaxial surfaces, dried and stored at −25 °C. Prior to inoculation, sporangia viability was confirmed by microscopic observations (Fig. S1) as described in Kortekamp et al. (2008). A suspension containing 10^4 sporangia ml^{-1} was used to spray the abaxial leaf surface, while controls were made by spraying the leaves with water (mock inoculations). After inoculation, plants were kept for 8 h in a moist chamber (100% humidity) and then kept under greenhouse conditions during the inoculation time course. The third to fifth fully expanded leaves below the shoot apex were collected at 6, 12, and 24 h post inoculation (hpi), immediately frozen in liquid nitrogen and stored at −80 °C. Three independent biological replicates were collected for each condition (inoculated and mock inoculated). Infection control was accessed 8 days after inoculation with the appearance of typicall disease symptoms (Fig. S2).

2.2. Metabolite extraction

Metabolite extraction from inoculated and mock inoculated grapevine leaves was adapted from a previous method (Maia et al., 2016). Metabolites were extracted using a solvent mixture methanol/water (2:1, v:v) in a ratio of 0.1 g of ground plant material to 1 mL of solvent. After adding the solvent mixture, samples were vortexed for 1 min and leucine enkephalin (YGGFL, Sigma Aldrich) was added to a final concentration of 0.25 μg/mL, mixture was vortexed again for 1 min. Samples were maintained in an orbital shaker for 15 min at room temperature and then centrifuged at 1000 *g* for 10 min and the supernatant was collected. Samples were immediately processed for analysis. Leucine enkephalin was used as internal calibrant, and the following m/z values were considered for analysis: $[M+H]^+ = 556.276575$ Th and $[M\text{-}H]^- = 554.2620221$ Th.

2.3. FT-ICR mass spectra acquisition

For each sample, the extracted methanol faction was diluted one thousand-fold in methanol for analysis by direct infusion, using electrospray ionization (ESI) in positive (ESI^+) and negative (ESI^-) modes as described previously (Maia et al., 2016). Mass spectra were acquired in a 7-T Apex Qe Fourier Transform Ion Cyclotron Resonance Mass Spectrometer (FTICR-MS, Brüker Daltonics) as previously described (Maia et al., 2016). Mass spectra were recorded in the mass range

between 100 and 1000 m/z (Fig. S3).

2.4. Untargeted metabolomic analysis by FT-ICR-MS

The software package Data Analysis 4.1 (Brüker Daltonics, Bremen, Germany) was used to compute the internal calibration of mass spectra (using leucine enkephalin for single point calibration). Mass peaks with a signal-to-noise ration of at least 4 were exported as peak lists to ASCII files. The alignment of the three biological replicates was performed using an in-house developed Python script by combining the peak lists into a peak matrix considering a tolerance of 1.0 ppm for mass deviations between samples, as previously described (Maia et al., 2016). For metabolite identification, the final mass list was submitted to MassTRIX 3 (Suhre and Schmitt-Kopplin, 2008) server (http://masstrix.org, accessed in June 2018) considering the following parameters: scan mode was positive or negative ionization; for the data obtained in positive ionization mode the adducts $M + H^+$, $M+K^+$ and $M + Na^+$ were considered; for negative ionization mode data, the adducts $M\text{-}H^+$ and $M + Cl^-$ were selected; a maximum m/z deviation of 2 ppm was considered; the organism *Vitis vinifera* was selected; search was performed in the databases "KEGG/HMDB/LipidMaps without isotopes". Differentially accumulated metabolites discrimination (Fold Change) between mock and inoculated samples were accessed through MetaboAnalyst 4.0 (Chong et al., 2018). The intensities of the annotated mass list were normalized using leucine enkephalin mass as reference. Missing value imputation was done by substitution by half of the minimum positive value found within the data. Intensity data generalized log transformed, and Pareto scaled prior to multivariate methods. Multivariate analysis, partial least squares - discriminant analysis (PLS-DA) was performed. The intensities of the most significant features of PLS-DA were also clustered by agglomerative hierarquical clustering using Euclidian distance as metric. Seeking the features most responsible for these differences, we obtained the top 15 of the most discriminatory peaks of the PLS-DA classification model by VIP score analysis. Obtained data were validated by Wilcoxon Rank Sum test ($p \leq 0.05$).

2.5. Compound annotation

Compounds were classified using the KEGG (Kyoto Encyclopedia of Genes and Genomes, http://www.genome.jp/kegg/) (Kanehisa et al., 2016; Ogata et al., 1999) database classification, except lipids, for which the LIPID MAPS (Lipidomics Gateway, http://www.lipidmaps.org/) (Sud et al., 2007) classification was considered. For each putative identified metabolite, an initial conversion of HMDB (Human Metabolome Database) to KEGG identifiers was performed using the "Linked entries option" option in the KEGG REST Service (http://rest.genome.jp/link/compound/hmdb). For lipid annotation, KEGG identifiers with LIPID MAPS correspondence were also converted using the "Linked entries option" (http://rest.genome.jp/link/compound/lipidmaps). Metabolite annotation into classes was performed by an in-house Python script, which uses the REST services of KEGG and LIPID MAPS Structure Database, using the KEGG and the LIPID MAPS identifiers as input, respectively. Finally a LIPID MAPS to KEGG conversion was performed and all KEGG identifiers containing KNApSAcK (Nakamura et al., 2014) (http://kanaya.naist.jp/KNApSAcK/) equivalencies were searched for their presence in the Plantae Kingdom. For compounds with multiple annotations a manual curation was performed. The analysis pipeline is presented in Fig. S4 and putative compound identification and annotation in Table S1.

2.6. RNA extraction and cDNA synthesis

Total RNA was isolated from inoculated and mock inoculated samples using the Spectrum™ Plant Total RNA Kit (Sigma-Aldrich, USA) and the residual genomic DNA was hydrolysed with the On-Column DNase I Digestion Set (Sigma-Aldrich, USA) as indicated by the manufacturer. RNA concentration and purity were determined at 260/280 nm using a NanoDrop-1000 spectrophotometer (Thermo Scientific), while its integrity was analysed by agarose gel electrophoresis. Prior to complementary DNA (cDNA) synthesis, all samples were analysed for genomic DNA contamination through a quantitative real time Polymerase Chain Reaction (qPCR) of a reference gene on crude RNA (Vandesompele et al., 2002). cDNA was synthesized from 2.5 µg of total RNA using RevertAid® H Minus Reverse Transcriptase (Fermentas, Ontario, Canada) anchored with Oligo $(dT)_{23}$ primer (Fermentas, Ontario, Canada), following the manufacturer's instructions.

2.7. Quantitative real time PCR

Based on the putatively identified compounds, metabolic pathways were built with the KEGG Mapper – Search & Color Pathway (http://www.kegg.jp/kegg/tool/map_pathway2.html), using the KEGG identifiers. The selection of genes for qPCR analysis was based on the biochemical pathways identified: *Lipoyl Synthase* (*LipA*) was selected as coding end enzyme for the lipoic acid biosythesis and *Palmitoyl-acyl carrier protein thioesterase* (*FatB*) was selected as related to palmitic acid (16:0) biosynthesis. For the flavonoid biochemical pathway, *Flavonol Synthase/Flavanone 3-hydroxylase* gene family (*FLS A, B, C, D, E* and *F*), *Flavonoid-3,5′-hydroxylase* (*F3′5′H*) and *Dihydroflavonol Reductase* (*DFR*) were selected for analysis (Table S2).

qPCR experiments were performed using the Maxima™ SYBR Green qPCR Master Mix (2 ×) kit (Fermentas, Ontario, Canada) following manufacturer's instructions. Each set of reactions included a control without cDNA template. Reactions were performed in the StepOne™ Real-Time PCR system (Applied Biosystems, Sourceforge, USA).

For all genes, thermal cycling started with a 95 °C denaturation step for 10 min followed by 40 cycles of denaturation at 95 °C for 15 s and annealing for 30 s. Dissociation curve analysis was performed to confirm single product amplification and the existence of non-specific PCR products (Fig. S5). Three biological replicates and two technical replicates were used for each sample. Gene expression (fold change) was calculated as described in Hellemans et al. (2007). *Elongation Factor 1-alpha* (*EF1α*), *Tetratricopeptide repeat protein 7B* (*TPR7B*) and *SAND family* (*SAND*) were used for expression data normalization as previously described (Monteiro et al., 2013).

2.8. Photosynthetic pigments extraction and quantification

Photosynthetic pigments were extracted from inoculated and mock inoculated ground leaves by adding 1.5 mL of methanol to 20 mg of plant material, and incubated in the dark at 4 °C for 48 h. Samples were centrifuged at 1200 *g* for 5 min and the supernatant was collected. The absorbance was measured at 470, 652.4 and 665.2 nm and the pigment's concentration for chlorophyll *a* (Chl*a*), chlorophyll *b* (Chl*b*) and total carotenoids was determined as previously described (Lichtenthaler, 1987).

2.9. Sugar extraction and quantification

Samples [0.1–0.2 mg fresh weight (FW)] were dried for 48 h at 70 °C and weighted to calculate the water content and dry weight (DW). Ethanol (80%, v/v) was added to each sample (1/10, g DW/v) and homogenized for 5 min. Samples were heated to 80 °C for 30 min and centrifuged at 16000 g for 15 min (Guy et al., 1992). Supernatant was collected, dried overnight at 70 °C and used to measure soluble sugars after re-suspension in water (1 mL). Pellet was dried overnight at 70 °C and used to measure starch (insoluble sugars). Sucrose concentration was measured by adding 0.25 mL of resorcinol (1%) and 0.75 mL of HCL (30%, v/v) to 0.1 mL of each sample. Samples were kept at 100 °C for 10 min. Reducing sugars concentration was determined by adding

1 mL of dinitrosalicylic acid (DNS) (0.25g DNS in 2 M NaOH) to 0.1 mL of each sample. Samples were kept at 80 °C for 8 min. Absorbance was measured at 470 and 520 nm for sucrose and reducing sugars, respectively (Almeida et al., 2007). The starch in dried pellet was submitted to acid hydrolysis, as previous described (Sebastiana et al., 2017), samples were centrifuged for 10 min at 15000 *g* and supernatant collected. Measurements of released D-Glucose were performed as described above for reducing sugars.

2.10. Determination of H_2O_2 content

H_2O_2 content was determined, as described by Childs & Bardsley (Childs and Bardsley, 1975) based on the oxidation of the chromogen 2′,2-azino-di (3-ethyl-benzathiazoline-6-sulphonic acid) catalyzed by a peroxidase in the presence of H_2O_2. Briefly, 100 mg of plant material were homogenized in a phosphate buffered saline solution (PBS) with 1–4% (w/v) of insoluble polyvinylpolypyrrolidone ($PVPP_{40000}$). Samples were centrifuged at 16000 *g* for 1 min and the supernatant was collected and used for the assay. Concentration of hydrogen peroxide (H_2O_2) was measured spectrophotometrically at 405 nm using a standard curve with known concentrations of H_2O_2. Three biological replicates and two technical replicates were used.

2.11. Antioxidant capacity assay

Total antioxidant capacity was measured spectrophotometrically at 405 nm using the antioxidant assay kit (Sigma-Aldrich), according to manufacturer's instructions. A standard curve with known concentrations of Trolox (Sigma-Aldrich) was used and data were normalized by protein content. Three biological replicates and two technical replicates were used.

2.12. Lipid peroxidation

For lipid peroxidation analysis, the thiobarbituric acid (TBA) assay was used (Hodges et al., 1999). Briefly, 100 mg of frozen samples were homogenized in ethanol 80% (v/v) and centrifuged at 14000 *g* for 5 min at 4 °C. The supernatants reacted with TBA solution at 95 °C for 30 min. Absorbance at 440, 532 and 600 nm was determined after a 10 min centrifugation at 14000 *g*, 4 °C. Malonaldehyde (MDA) equivalents (nmol ml^{-1}) = [(A − B) × 106]/157 000, where A = [[(Abs532 + TBA) − (Abs 600 + TBA)] − [(Abs 532 − TBA) − (Abs 600 − TBA)]] and B = [[(Abs 440 + TBA) − (Abs 600 + TBA)] × 0.0571].

2.13. Statistical analysis

Two-sample statistical differences in expression and biochemical data was assessed by the Mann-Whitney *U* test implemented in IBM® SPSS® Statistics software (version 23.0; SPSS Inc., USA). Results yielding $p < 0.05$ were considered statistically significant.

3. Results

3.1. Vitis vinifera cv. Trincadeira inoculated with P. viticola and control samples present distinct metabolic profiles

The compatible host–pathogen interaction between *Vitis vinifera* cv. Trincadeira plants, inoculated with *P. viticola* at 6, 12 and 24 hpi, was characterized using an untargeted metabolomics approach (Fig. 1, Fig. S3). Differences in the metabolic content of healthy and infected samples, particularly at 12 hpi, are seen through the comparison of mass spectra obtained for control leaf and its corresponding infected sample (Fig. 1).

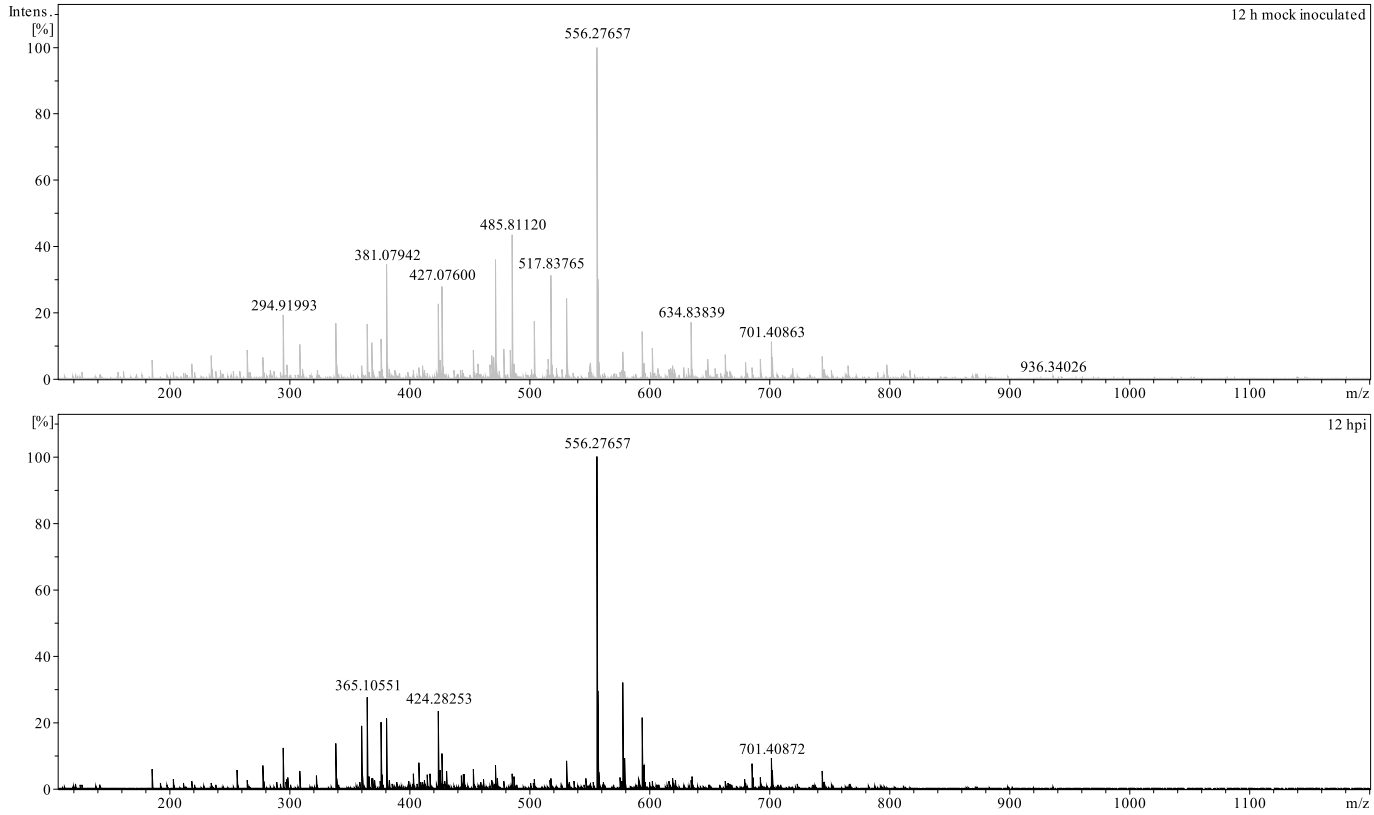

Fig. 1. Cumulative mass spectra of *Vitis vinifera* cv Trincadeira interaction with *P. viticola* at 12 hpi. Data were acquired in positive (ESI+) electrospray mode performing direct infusion analysis in the range 100–1100 m/z. The software DataAnalysis 4.1 was used for the creation of mass spectra. Control samples are represented in gray and inoculated samples are represented in black.

From the initial total of 11406 ion peaks detected in both positive and negative ionization modes, a total of 1460 putative metabolites belonging to various chemical groups were putatively or tentatively identified (Table 1).

A data matrix considering only the masses putatively assigned to a metabolite was submitted to MetaboAnalyst 4.0 for statistical analysis. Application of the multivariate analysis PLS-DA revealed a separation between inoculated and control samples at all of the studied time-points and both ESI modes (Fig. 2 - A, B) indicating that the response to pathogen attack influences the metabolic profile of the host. Samples within each individual class upon inoculation clustered tightly with a higher separation at 24 hpi. VIP score analysis (Fig. 2 - C, D) allowed the identification of masses that contributed more to the PLS-DA model and the association to control or inoculated samples.

A total of 72 m/z putatively annotated metabolites presented significant modulation ($p \leq 0.05$) between inoculated and control samples at each time-point. As illustrated on Fig. 3, the predicted metabolites from the mass peaks are associated with a small number of distinct areas of metabolism, the most predominant of which involved lipid, carbohydrate, aromatic, alkaloid and organic acids metabolism. Full lists of putative signal annotations are given in Table S1. In view of the exceedingly small contribution of *P. viticola* hyphae to overall biomass at the early time-points of inoculation, it is likely that the majority of extracted metabolites are of plant origin. We have further conducted queries on the comprehensive Species-Metabolite Relationship Database (KNApSAcK) and confirmed that the putative identified metabolites were indeed assigned to the Plant Kingdom (Table S1).

3.2. Lipid modulation after P. viticola inoculation

Along inoculation time course, lipids was the metabolic class most modulated. Within this class, From the three time-points analysed, lipids was the one showing the greatest differences fatty acyls were the most affected, followed by glycerophospholipids, prenol lipids, glycerolipids, polyketides, sterol lipids and sphingolipids.

Overall, on the first 24 h of interaction, there was a negative modulation of most lipids classes when compared to the non-inoculated control samples (Fig. 4). Fatty acyls and polyketides were the classes that presented more lipids with increased concentration, being their accumulation more evident at 6hpi.

3.3. Changes in the content of carbohydrates and photosynthetic pigments after P. viticola inoculation

Photosynthesis allows the conversion of carbon dioxide into sugars which were unsurprisingly detected in the leaf extracts by FTICR-MS. However, a limitation of this methodology is the inability to distinguish between isomers, which are very common among carbohydrates (Table S1). The majority of the identified carbohydrates are down-accumulated; with exception of the m/z 543.13205 $[M + K39]^+$ putatively assigned to the raffinose family of oligosaccharides (RFOs) up-accumulated at 6 hpi and the m/z 322.99374 $[M-H]^-$ putatively assigned to fructose 1,6-bisphosphate at 12 hpi.

We have further quantified glucose, fructose, sucrose and starch as well as the major pigments (Chl*a*, Chl*b* and carotenoids) as photosynthesis biomarkers. Reducing sugars in inoculated samples presented a 2-fold increase at 6 hpi (mock inoculated: 109.24 ± 9.55 mg g^{-1} DW; inoculated: 212.45 ± 43.98 mg g^{-1} DW). At 12hpi an increase in starch concentration was also observed in inoculated samples (mock inoculated: 99.44 ± 3.38 mg g^{-1} DW; Inoculated: 144.52 ± 0.38 mg g^{-1} DW) (Table 2). At 24hpi, no significant changes on non-structural carbohydrate content occurs. Photosynthetic pigments showed no significant variation in the first 24 h of infection suggesting no variation in photosynthesis rate (Fig. S6).

3.4. Oxidative stress, lipid peroxidation and antioxidant capacity

One of the metabolic classes with higher changes in Trincadeira after pathogen inoculation is the lipids class. Lipids may be altered by Reactive oxygen species (ROS) that are produced after pathogen contact, as higher ROS content has the capacity to fragment the fatty acids within the membranes into structurally diverse products that may act as signaling molecules (Walley et al., 2013). Thus, we further evaluated H_2O_2 production, lipid peroxidation and antioxidant capacity at 6, 12 and 24 hpi.

At 6 and 12hpi there is an increase of H_2O_2 concentration (6 h: 0.215 ± 0.12 μmol g^{-1} FW, 6 hpi: 0.557 ± 0.09 μmol g^{-1} FW; 12 h: 0.200 ± 0.141 μmol g^{-1} FW, 12 hpi: 0.741 ± 0.09 μmol g^{-1} FW). After inoculation with *P. viticola*, lipid peroxidation also increased (6 h: 9.035 ± 1.011 nmol MDA g^{-1} FW, 6 hpi: 27.607 ± 2.370 nmol MDA g^{-1} FW; 12 h: 16.586 ± 3.449 nmol MDA g^{-1} FW, 12 hpi: 30.591 ± 4588 nmol MDA g^{-1} FW; 24 h: 12.062 ± 3.503 nmol MDA g^{-1} FW, 24 hpi: 34.111 ± 6.031 nmol MDA g^{-1} FW). The antioxidant capacity remained unaltered in all the time-points analysed (Fig. 5).

3.5. Metabolic pathways and gene expression analysis

We have selected fatty acyls and polyketides lipid classes to further evaluate the expression of some genes coding for key enzymes of the biosynthetic pathways of compounds that represent metabolic class modulation. Lipoic acid (m/z 205.03623 $[M-H]^-$) and palmitic acid derivatives (m/z 339.19448 $[M+H]^+$) belong to the fatty acyls class within lipids. Fatty acids metabolites were mainly down-accumulated after pathogen inoculation. *Lipoyl Synthase* (*LipA*) and *Palmitoyl-acyl carrier protein thioesterase* (*FatB*) were selected as coding enzymes for on lipoic acid and palmitic acid biosynthesis.

We have also selected flavonoids (polyketides) to be further analysed. Flavonoids were previously reported to play an important role in plant defense mechanisms against pathogens (reviewed in Mierziak et al., 2014). While this metabolic class is negatively regulated, one flavonoid putatively identified as ulexone B (m/z 425.13612 $[M+Na]^+$) is highly accumulated at 6, 12 and 24 hpi (over 20 fold). The biochemical pathway for flavonoid biosynthesis was analysed (Fig. S7) and genes coding for the enzymes flavonol synthase/flavanone 3-hydroxylase (*FLS A, B, C, D, E* and *F*), dihydroflavonol reductase (*DFR*) and flavonoid-3,5′-hydroxylase (*F3′5′H*) were selected for expression

Table 1
Number of peaks, identified compounds and differently accumulated metabolites identified with ESI(+) and ESI(−) at 6, 12 and 24 h after inoculation.

Time Points	Peaks		Identified masses		Differently accumulated	
	Ionization Mode					
	ESI(+)-MS	ESI(−)-MS	ESI(+)-MS	ESI(−)-MS	ESI(+)-MS	ESI(−)-MS
6hpi	2512	1318	264	145	11	10
12hpi	1365	1331	247	160	15	8
24hpi	3726	1154	520	124	21	12
Total	11406		1460		77	

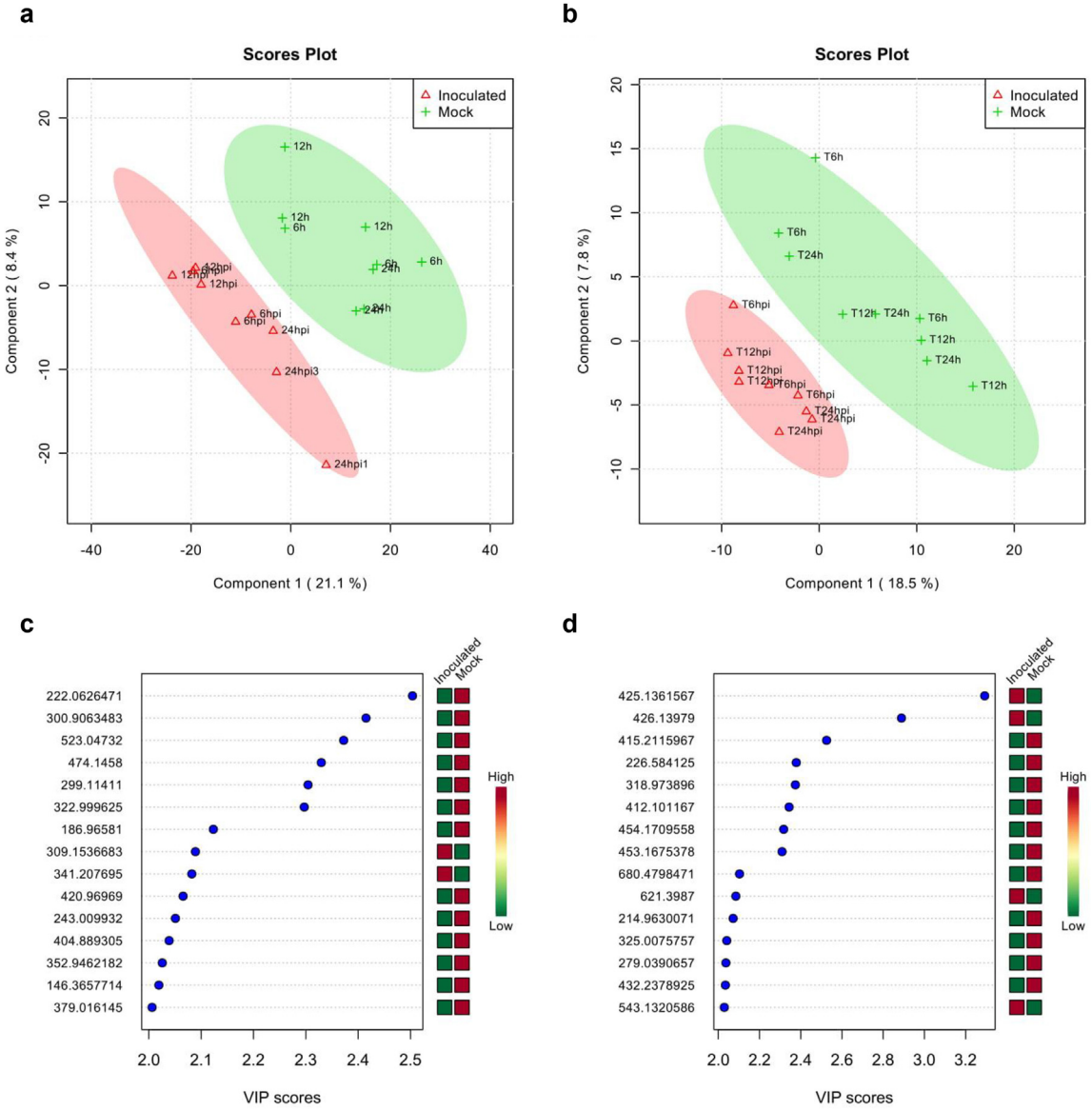

Fig. 2. Partial least squares-discriminant analyses (PLS-DA) PC1/PC2 score plots and variable's importance (VIP scores) of secondary metabolite profiles of *Vitis vinifera* cv. Trincadeira at 6, 12 and 24 hpi with *P. viticola.*
(A) PLS-DA score plot of ESI(−) samples; (B) PLS-DA score plot of ESI(+) samples; (C) VIP scores of Component 1 in ESI(−); (D) VIP scores of Component 1 in ESI (+). In the score plots, the ellipse represents the Hotelling T2 with 95% confidence interval. Three biological replicates were performed per analysis.

analysis.

FatB was up-regulated only at 24 hpi (4.0 ± 0.15 fold-change) while *Lip A* remained unaltered (6 hpi: 1.3 ± 0.2, 12 hpi: 1.3 ± 0.4, 24 hpi: 1.2 ± 0.2 fold-change). *Flavonol Synthase/Flavanone 3-hydroxylase* comprises several genes in grapevine. We have analysed the expression of 6 *FLS* genes. The majority of the genes were strongly down-regulated (*FLS-A*: −3.4 ± 0.99 to −14.6 ± 2.4 fold-change; *FLS-D*: −6.4 ± 4 to −20.1 ± 1.8 fold-change; *FLS-E*: −2.7 ± 0.5 to 1.36 ± 0.1 fold change) or even undetected on the inoculated samples (*FLS-B* and *FLS-C*). *Flavonoid-3,5′-hydroxylase* (F3′5′H) expression was not altered at 6 and 12 hpi and increased at 24 hpi (5.15 ± 0.38 fold-change). *Dihydroflavonol reductase* expression was not significantly altered after pathogen challenge, despite being down-regulated at 6 hpi (Fig. 6).

4. Discussion

Plasmopara viticola is a strictly biotrophic oomycete pathogen, which can only survive on tissues of its natural host. Despite being a widely studied interaction, the characterization of the first hours after pathogen challenge on compatible interactions has been poorly studied. It is believed from other pathosystems that *P. viticola* may suppress host defenses through the secretion of effector molecules that impair grapevine defense mechanisms. Also, *Vitis vinifera* susceptibility to *P. viticola* suggests that this specie does not present an effective pathogen recognition system that allows a full activation of a defense system to successfully restrain pathogen growth (Gaspero et al., 2007). However, several studies indicate the presence of a weak defense mechanism with a transient activation of defense-related genes and proteins (Figueiredo et al., 2017, 2012; Hamiduzzaman et al., 2005; Kortekamp, 2006; Milli et al., 2012; Polesani et al., 2010) that is neither fast nor robust enough to prevent the pathogen from spreading.

Mechanisms associated with compatibility and disease development were shown to be established later at the oil-spot stage where grapevine transcripts from all major functional categories, including defense processes were strongly down-regulated and genes related to

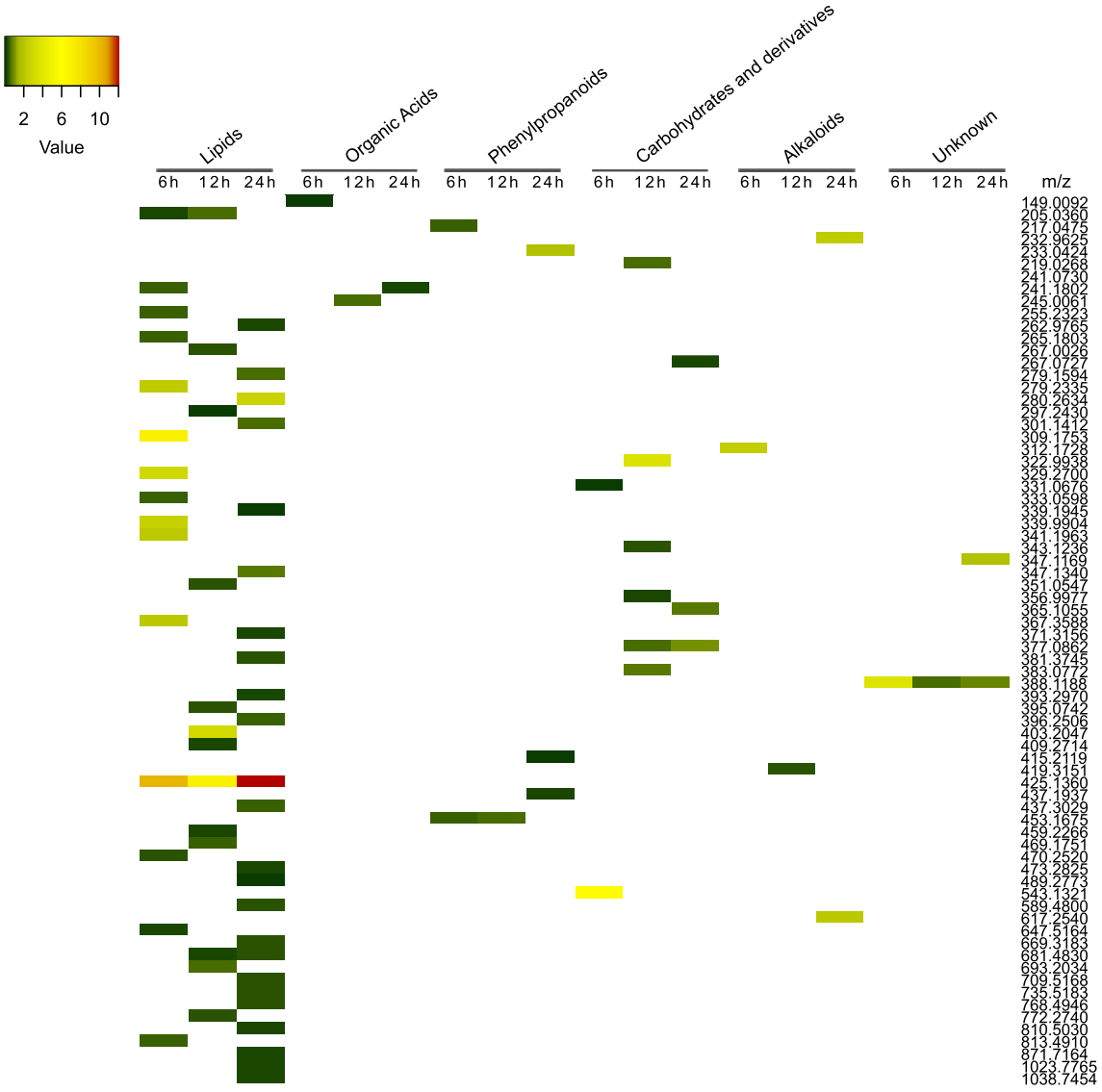

Fig. 3. Heatmap of differently accumulated features on each metabolic class.
Each column indicates the metabolic major class and time-point (6, 12, and 24 hpi). Each row represents a feature (m/z) putatively identified as a metabolite in Trincadeira. Coloring indicates differential accumulation between inoculated and control samples: dark green indicates low accumulation (fold change < 1), light green to yellow indicates a fold change between 2 and 10 and orange to red indicates high accumulation (fold change > 10).

carbohydrate transport and partitioning were activated (Hayes et al., 2010; Polesani et al., 2008).

At the metabolic level, changes on both primary and secondary metabolisms were shown to occur after *P. viticola* interaction and few metabolic markers were described for both compatible and incompatible interactions (Ali et al., 2009; Batovska et al., 2009; Buonassisi et al., 2017; Chitarrini et al., 2017). We have previously assessed the metabolic modulation of tolerant and susceptible grapevine cultivars at early time-points of *P. viticola* inoculation by ^{1}HNMR and shown that the compatible interaction is characterized by a significantly higher accumulation of glucose, glutamic acid and succinic acid on the first hours of interaction (Ali et al., 2012). To further investigate the metabolic changes of the compatible interaction between grapevine and *P. viticola* we have conducted a high-throughput metabolome characterization of challenged Trincadeira plants with *P. viticola* during the early infection (6, 12 and 24 hpi), as well as comparable uninfected controls. Our data shows that the abundance of several metabolites decreased relative to mock inoculation during the first hours after inoculation which is in accordance to the previously described for wheat compatible interaction (Gunnaiah and Kushalappa, 2014). At 6hpi, 21 putative metabolites were modulated, 23 at 12hpi and 33 at 24hpi, being lipids and carbohydrates the most affected metabolic classes.

4.1. Lipid metabolism is mostly affected by P. viticola in the first hours of inoculation

Besides structural functions, lipids are also associated to transport of other compounds in membranes, protection of plants to abiotic and biotic stresses, extracellular and intracellular signaling and storage of energy (Dufourc, 2008; Fahy et al., 2011; Horn and Chapman, 2014; Hou et al., 2016; Laloi et al., 2007; Shah, 2005; Zauber et al., 2014). In the present work, after pathogen challenge, over half of the putatively identified metabolites affected in Trincadeira were annotated as lipids (Fig. 3 and Table S1). Within lipids, fatty acyls (FA) was the most represented class, at 6hpi several FA were more accumulated in the inoculated plants, while on both 12 and 24hpi there was a decrease of FA accumulation (Fig. 4). As an obligatory biotroph, *P. viticola*'s early steps of infection establishment are the adhesion to the plant surface, germination and the differentiation of penetration structures, after which

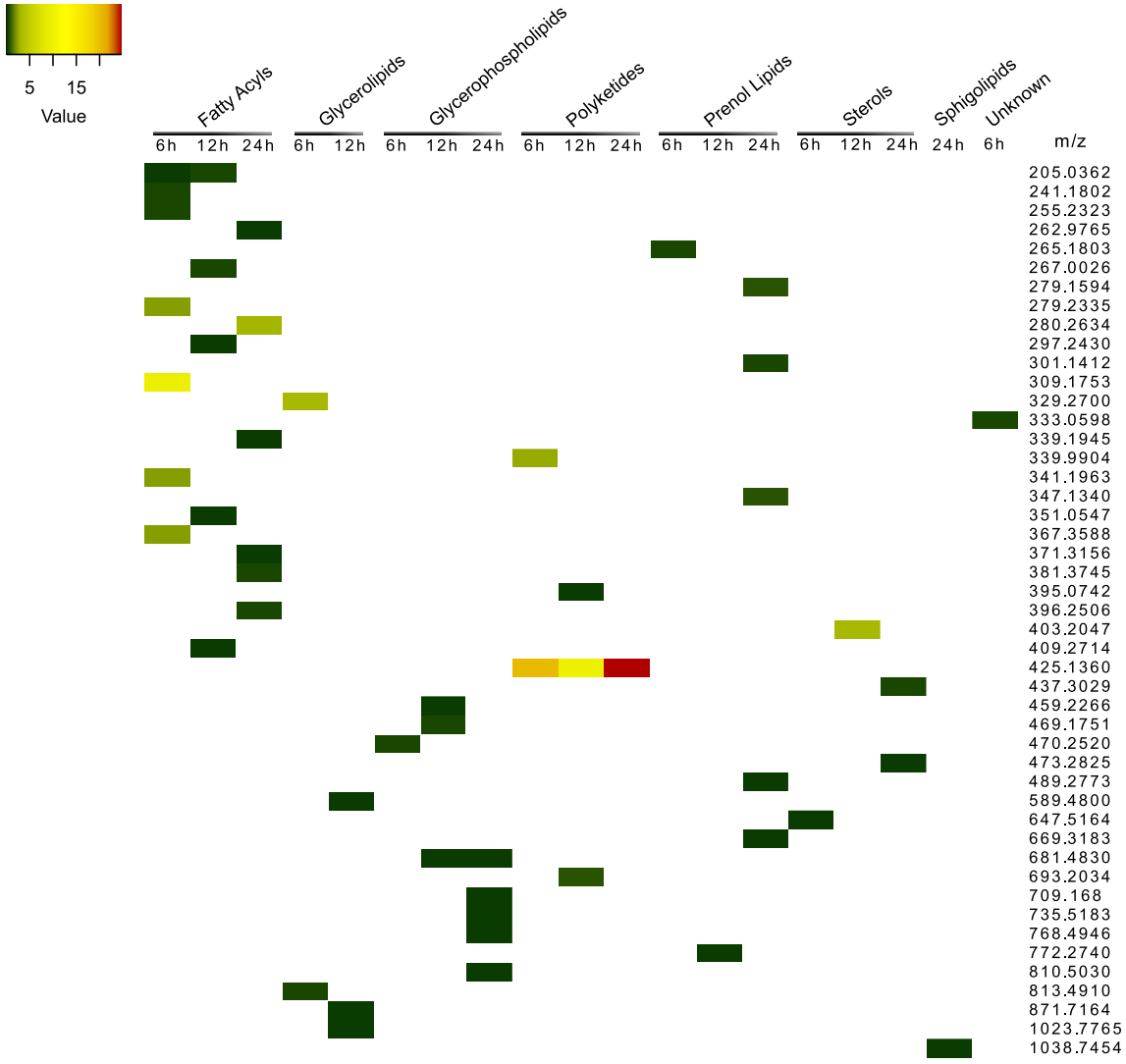

Fig. 4. Heatmap of differently accumulated features on secondary lipid classes.
Each column indicates the secondary lipid class and time-point (6, 12, and 24 hpi). Each row represents a feature (m/z) putatively identified as lipid in Trincadeira. Coloring indicates differential accumulation between inoculated and control samples: dark green indicates low accumulation (fold change < 1), light green to yellow indicates a fold change between 2 and 10 and orange to red indicates high accumulation (fold change > 10).

Table 2
Reducing sugars, sucrose and starch quantification in control and inoculates. Results in mg sugar g−1 DW. * Statistically significant differences between the inoculated and control replicates ($p \leq 0.05$; Mann-Whitney *U* test).

		6 hpi	12 hpi	24 hpi
Reducing Sugars	Control	109.24 ± 9.55	159.81 ± 2.53	112.57 ± 8.66
	Inoculated	**212.45 ± 43.98***	143.09 ± 22.43	131.92 ± 27.91
Sucrose	Control	50.42 ± 4.69	39.64 ± 4.25	26.60 ± 7.61
	Inoculated	44.74 ± 5.99	38.59 ± 6.30	38.49 ± 5.76
Total Soluble Sugars (TSS)	Control	159.66 ± 13.81	199.45 ± 6.78	139.17 ± 5.12
	Inoculated	**257.19 ± 49.66***	181.68 ± 28.14	170.40 ± 31.72
Starch	Control	87.59 ± 1.93	99.44 ± 3.38	119.33 ± 5.68
	Inoculated	93.08 ± 7.09	**144.52 ± 0.38***	115.37 ± 21.12
Total non-structural sugars (TS)	Control	247.26 ± 13.47	298.89 ± 10.16	258.50 ± 6.59
	Inoculated	350.26 ± 55.93	326.20 ± 27.77	285.78 ± 27.81

they colonize plant tissues by several different routes: their hyphae may spread over the plant cuticle, under the cuticle, between host cells or inside host cells (reviewed in O'Connell and Panstruga, 2006). During these plant-pathogen interactions, fatty acyls and plant derived fatty acids play an important role in the both pathogen recognition, activation of plant defenses and induction of systemic acquired resistance (Lim et al., 2017; Walley et al., 2013). The FA species most accumulated at 6hpi were putatively assigned to the fatty acids linoleic (18:2) and tetracosanoic or lignoceric acid (m/z 279.23350 $[M-H]^-$ and m/z 367.35883 $[M-H]^-$), to α-chloro chain fatty aldehydes as 2-chlorohexadecanal (m/z 309.17530 $[M + Cl35]^-$) and to eicosanoids (m/z 341.19631 $[M-H]^-$). Although accumulation of 18:2 was shown to elicit

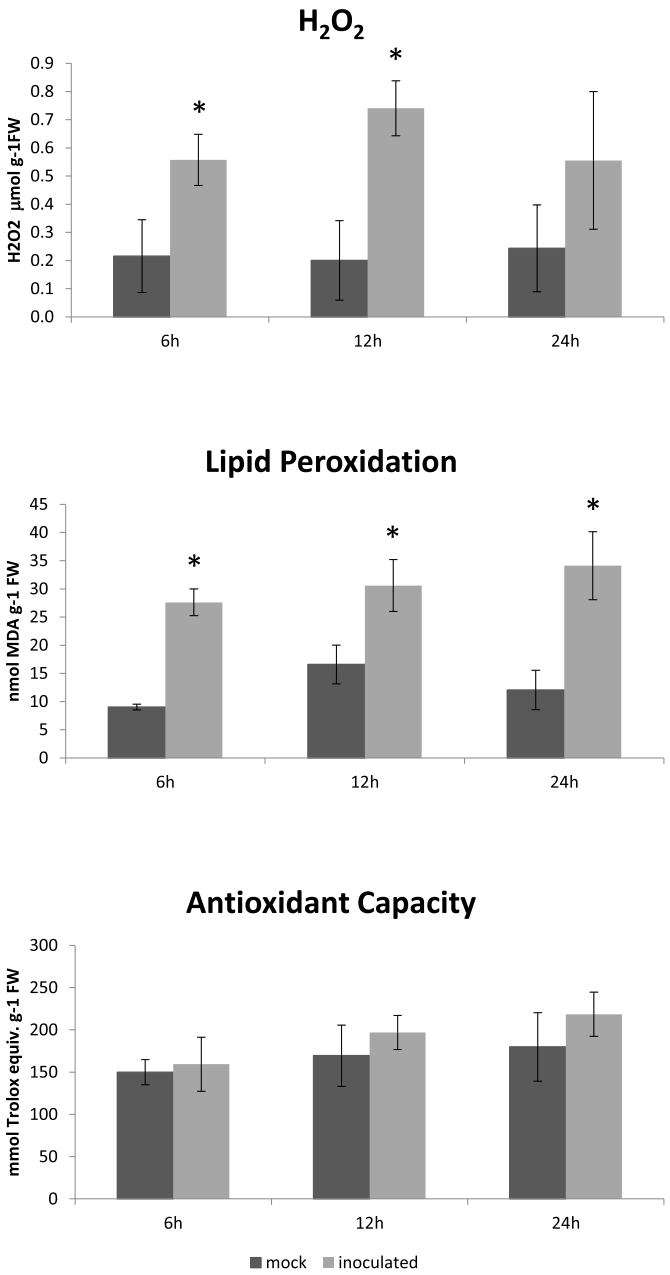

Fig. 5. ROS production, lipid peroxidation and antioxidant capacity in *V. vinifera* cv Trincadeira inoculated leaves with *P. viticola* at 6, 12 and 24 hpi. (a) Hydrogen peroxide (µmol Hydrogen peroxide g^{-1} Fresh Weight (FW)); (b) MDA content (nmol MDA equiv. g^{-1} FW); (c) total antioxidant capacity (µmol Trolox equiv. mg^{-1} protein). * represents statistically significant differences between the inoculated and control replicates ($p \leq 0.05$; Mann-Whitney *U* test).

enhanced resistance to attack by the fungal pathogen, *Colletotrichum gloeosporioides* (Madi et al., 2003), on grapevine-*P. viticola* interaction we have previously shown that one major feature differentiating the compatible from the incompatible interaction is the linolenic acid (18:3) accumulation, followed by jasmonic acid (JA) synthesis in the incompatible interaction. We have shown that the expression of the genes coding for main enzymes of JA biosynthetic pathway (*LOX2, AOC, AOS, OPR3*), JA-Ile conjugation (*JAR1*) and JA-Ile receptor (*COI1*) are down-regulated in Trincadeira at 6, 12 and 24 hpi (Ali et al., 2012; Guerreiro et al., 2016; Figueiredo et al., 2017) suggesting that oxilipin synthesis is not activated.

Also, α-chloro chain fatty aldehydes, in particular 2-chlorohexadecanal, have been described in humans as related to potentially pro-inflammatory effects ranging from direct toxicity to inhibition of nitric oxide synthesis (Ford, 2010). Moreover, it was described that 2-chlorohexadecanal could elicit functional changes in targeted cells through Schiff base adduct formation with primary amines of proteins and lipids. Schiff base adduct formation could potentially alter membrane dynamics and protein function, thus eliciting cell injury or mediating signaling pathways (Ford, 2010).

Lipoic acid is a mitochondrial coenzyme that is essential for the activity of enzyme complexes such as those of pyruvate dehydrogenase and glycine decarboxylase, it also acts as chemical antioxidant (Yi and Maeda, 2005). No expression changes on *LipA* suggest that lipid acid decrease in the inoculated samples may be due to its role on ROS detoxification.

Also, flavonoids within polyketides lipid class were affected on the first hours of interaction. While overall this metabolic class is negatively affected with exception of m/z 425.13612 $[M+Na]^+$ putatively identified as ulexone B, showing a 20-fold increase at 6, 12 and 24 hpi. This flavonoid was previously pinpointed for its potential contribution to fusarium head blight (FHB) (Gunnaiah and Kushalappa, 2014) resistance. Flavonoids have been previously described to be very important in plant resistance against fungi (Mierziak et al., 2014). In plant pathogen interactions, it has been suggested that constitutive flavonoids are able to slow down pathogen development, by the accumulation of high amounts of flavonoids on the site of infection and inducing a hypersensitivity reaction (Mierziak et al., 2014).

In grapevine, the accumulation of constitutive flavonols is able to decreased grapevines susceptibility to downy mildew (Agati et al., 2008; Latouche et al., 2013). We have further evaluated the expression of several *FLS* and *F3'5'H* coding genes. F3'5'H presented no significant expression modulation on the first hours of infection (6 and 12hpi), being up-regulated at 24hpi. *FLS* genes presented an overall down-regulation at early infection time-points, with exception of *FLS-F* that is positively modulated from 12hpi. Moreover, *DFR* was also down-regulated at 6 hpi, accordingly to the previously described for *Vitis vinifera* Riesling (susceptible genotype) on the first hours after inoculation with *P. viticola* (Kortekamp, 2006). The reprogramming of metabolic pathways is considered to be one of the defense strategies that plants utilize to generate antimicrobial compounds and signal molecules for restraining the growth of pathogens (La Camera et al., 2004). Our results suggest that on the first hours of inoculation, flavonoid metabolism is not activated to a greater extent and thus synthesis of secondary metabolites may not be promoted as a defense strategy so early after pathogen challenge. Our results are in accordance to the study of the susceptible *V. vinifera* cv Cabernet sauvignon inoculated with *Erysiphe necator*, where activation of flavonoid pathway genes occurs from 24 hpi (Fung et al., 2008).

4.2. Oxidative stress and fatty acid fragmentation are impaired on the first hours of the compatible grapevine-P. viticola interaction

Reactive oxygen species play an important role on plant-pathogen interactions. ROS have been suggested to be the first line of defense against pathogen invasion, either by directly killing the pathogen, or by slowing down its development by cell wall reinforcement through cross-linking of glycoproteins, lipid peroxidation and hypersensitive reaction and systemic defense signals propagation (Torres et al., 2006).

Normally, two phase kinetics of ROS accumulation are observed during plant-biotrophic fungi interaction: a first burst happens at early time-points of interaction in both resistant and susceptible plant hosts and a second burst that only occurs in the incompatible interaction (Gebrie, 2016).

In Trincadeira, a significant H_2O_2 increase occurred in inoculated samples when compared to non-inoculated samples at 6 and 12hpi, however H_2O_2 content was low when compared to the accumulation in tolerant genotypes as described previously (Figueiredo et al., 2017). This low H_2O_2 accumulation during the initial biotrophic phase of the

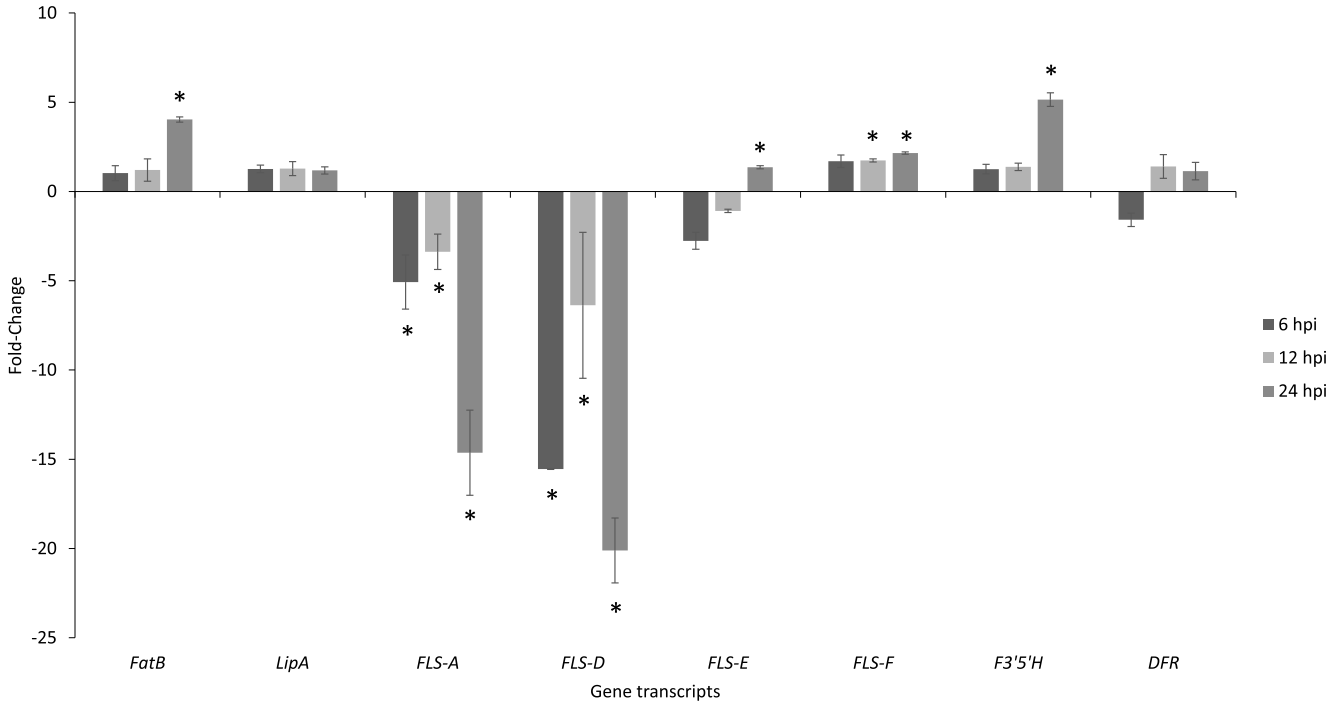

Fig. 6. Gene expression profile in inoculated leaves.
For each time point (6, 12 and 24 hpi) gene transcripts fold-change relative to controls are represented for *FatB, LipA, FLS-A*, FLS-*D, FLS-E, FLS-F, F3'5'H* and *DFR*. Fold-change values are relative to expression in mock leaves. * represents statistically significant differences between the inoculated and control samples ($p \leq 0.05$; Mann-Whitney *U* test).

interaction, where hyphae are growing into the host apoplast may not be sufficiently toxic to the pathogen and thus not being able to restrain pathogen growth.

MDA accumulation due to lipid peroxidation has been reported in response to a variety of abiotic and biotic stresses. The production of lipid peroxides has been shown to be induced by pathogens (Patel and Williamson, 2016). In Trincadeira, a significant MDA accumulation occurred after pathogen challenge, indicating disruption of cellular membrane and causing a loss of cellular integrity leading to further ROS generation. Moreover, the unaltered antioxidant capacity may also account for lipid peroxidation or oxidative stress in the susceptible cultivar. Thus there seems to be an attempt to activate the first line of defenses with a ROS burst Trincadeira, which is in accordance with other studies on compatible plant-pathogen interactions (Mandal et al., 2011; Supian et al., 2017). Very recently, a study on the biotrophic rice-*Magnospora oryzae* interaction has shown that the biotrophic pathogen secretes an AVR-Pii effector that accumulates at the biotrophic interfacial complex, is translocated into the invaded cytoplasm and neighboring cells. This effector disrupts ROS burst by suppressing NADPH production in susceptible rice cultivar. The pathogen is able to reprogram host metabolism to establish compatibility impairing ROS production. The AVR-Pii effector plays an essential role as one of the key pathogenicity determinants in disrupting host innate immunity (Singh et al., 2016). We hypothesize that *P. viticola* is able to control the first line of defense in Trincadeira on a similar manner.

4.3. Pathogen-driven modulation of host carbohydrate metabolism

Carbohydrate partitioning between plant source and sink tissues is influenced by pathogens. In fact, plants and pathogens evolved together in a constant battle in which the plant limits pathogen access to nutrients and initiates immune responses, whereas the pathogen evolves adaptive strategies to gain access to nutrients and suppress host immunity. In the case of a successful interaction, pathogens are believed to re-direct plant's metabolism to their own benefit. This comprises the suppression of plant defense responses and the reallocation of photoassimilates to sufficiently supply the pathogen with nutrients (reviewed in (Berger et al., 2007). In compatible host–biotroph interaction, a reduction in photosynthesis rate is commonly described for later infection time-points (Swarbrick et al., 2006). For the grapevine interaction with downy mildew a photosynthesis decrease on the oil spot stage was reported together with lower concentration of photosynthetic pigments around the oil spot lesion (Moriondo et al., 2005). However, data is scarce regarding grapevine carbohydrate metabolism modulation on the first hours of interaction with *P. viticola*. Our data shows that no alteration of photosynthetic pigments content occurred up to 24 hpi, suggesting that the photosynthesis rate remains unaltered at early inoculation time-points where there are no visible lesions or symptoms. The same was described for the biotroph interaction between barley and powdery mildew (Swarbrick et al., 2006). On the first days of interaction no significant difference in the rate of CO_2 assimilation between uninfected and infected leaves occurred but on latter time-points a decrease on CO_2 assimilation of infected susceptible leaves was shown (Swarbrick et al., 2006). Pathogens also affect plant sugar levels, but their effect varies considerably between different plant–pathogen interactions. In tomato leaves inoculated with the necrotroph *Botritis cinerea*, sucrose, glucose and fructose levels decreased after 3 days post inoculation (dpi) (Berger et al., 2004), while in barley leaves inoculated with powdery mildew, hexose and sucrose content increased after 3 dpi (Swarbrick et al., 2006). In Trincadeira, both the content of reducing sugars and total soluble sugars significantly increased in inoculated samples at 6hpi. The higher content on glucose is in accordance to our previous studies where we have compared by H^1NMR the metabolic modulation prior and after *P. viticola* inoculation (Figueiredo et al., 2008; Ali et al., 2012). On the first hours of interaction with the pathogen, Trincadeira was characterized by a higher level of glucose and sucrose as well as other organic acids such as glutamic acid, succinic acid and ascorbic acid when compared to the tolerant cultivar Regent (Ali et al., 2012). On the present study the levels of sucrose were not altered, being the higher amount of total soluble sugars, a result of

reducing sugars (mostly glucose and fructose in leaves) accumulation. Our results may indicate an allocation of photosynthetic fixed carbon to be quickly metabolized within the cells or to an immediate transport to sink tissues. This increase may also be influenced by the pathogen as at the early inoculation time-points, the pathogen has entered through the plant stomata and is forming the haustorium which requires an adequate nutrient supply (Gindro et al., 2003; Unger et al., 2007), thus despite the relatively small number of initially invaded epidermal cells, the pathogen may be able to modulate metabolism and metabolite transport in distant mesophyll and vascular tissues. At 12 hpi carbon allocation seems to be channelled to be stored in chloroplast as starch, and the carbon exported retained as fructose-1,6-bisphosphate in inoculated samples. On other hand, small disaccharides (RFOs) appear more accumulated at 6 hpi. They were previously shown to accumulate to a high extent in syncytia during nematode infection (Hofmann et al., 2010). The exact function of RFO on biotic interactions is not known, although it has previously described that RFOs may act as osmolytes to maintain cellular integrity and function under oxidative stress conditions (Nishizawa et al., 2008; Nishizawa-Yokoi et al., 2008). Also the higher ratio hexoses/sucrose found 6 hpi contributes to osmotic adjustment. Presence of a raffinose transporter in chloroplast membrane has been established, although whether they help in maintaining chloroplast membrane integrity under oxidative stress, is not known (Schneider and Keller, 2009).

5. Conclusions

Overall, there was a negative modulation of several metabolic classes associated to pathogen defense such as flavonoids or phenylpropanoids. Despite a H_2O_2 burst and lipid peroxidation were detected, H_2O_2 levels during the initial biotrophic phase of the interaction may not be sufficiently toxic to the pathogen to restrain its growth. Photosynthesis rate seems to be unaffected on the first hours of interaction but an early modulation of the carbohydrate metabolism that may be associated to pathogen nutrition on the first colonization steps occurs. Other challenges that require future attention are associated to the interaction between *P. viticola* effectors and host plant mechanisms. *P. viticola* genome was recently sequenced opening new insights into effectors and pathogenicity factors that may contribute for *P. viticola* virulence leading to the establishment of a compatible interaction. Further studies may provide a better understanding of this interaction allowing the development of new and sustainable disease control measures.

Author contribution

AF and MSS conceived the study and performed the experimental design. RN, MM and MSS performed the FTICR-MS and expression analysis experiments. RN and ABS performed sugar quantification. RN, AENF, MM, CC, MSS, AF and MM performed data analysis. RN, MM and AF wrote the manuscript. All authors have revised the manuscript. The authors declare that the research was conducted in the absence of any commercial or financial relationships that could be construed as a potential conflict of interest.

Acknowledgments

This work was supported by Fundação para a Ciência e a Tecnologia, FCT/MCTES/PIDDAC, Portugal through the projects PEst-OE/BIA/UI4046/2014, UID/MULTI/00612/2013, investigator FCT program IF/00819/2015 to AF and PhD grant PD/BD/116900/2016 to MM. We acknowledge the support from the Portuguese Mass Spectrometry Network (LISBOA-01-0145-FEDER-022125) and the European Project EU_FT-ICR_MS (H2020-INFRAIA-02-2017).

Appendix A. Supplementary data

Supplementary data to this article can be found online at https://doi.org/10.1016/j.plaphy.2019.01.026.

References

Agati, G., Cerovic, Z.G., Marta, A.D., Stefano, V.D., Pinelli, P., Traversi, M.L., Orlandini, S., 2008. Optically-assessed preformed flavonoids and susceptibility of grapevine to Plasmopara viticola under different light regimes. Funct. Plant Biol. 35, 77–84. https://doi.org/10.1071/FP07178.

Ali, K., Maltese, F., Figueiredo, A., Rex, M., Fortes, A.M., Zyprian, E., Pais, M.S., Verpoorte, R., Choi, Y.H., 2012. Alterations in grapevine leaf metabolism upon inoculation with *Plasmopara viticola* in different time-points. Plant Sci. 191–192, 100–107. https://doi.org/10.1016/j.plantsci.2012.04.014.

Ali, K., Maltese, F., Zyprian, E., Rex, M., Choi, Y.H., Verpoorte, R., 2009. NMR Metabolic Fingerprinting Based Identification of Grapevine Metabolites Associated with Downy Mildew Resistance. J. Agric. Food Chem. 57, 9599–9606. https://doi.org/10.1021/jf902069f.

Almeida, A.M., Silva, A.B., Araújo, S.S., Cardoso, L.A., Santos, D.M., Torné, J.M., Silva, J.M., Paul, M.J., Fevereiro, P.S., 2007. Responses to water withdrawal of tobacco plants genetically engineered with the AtTPS1 gene: a special reference to photosynthetic parameters. Euphytica 154, 113–126. https://doi.org/10.1007/s10681-006-9277-2.

Armijo, G., Schlechter, R., Agurto, M., Muñoz, D., Nuñez, C., Arce-Johnson, P., 2016. Grapevine Pathogenic Microorganisms: Understanding Infection Strategies and Host Response Scenarios. Front. Plant Sci. 7. https://doi.org/10.3389/fpls.2016.00382.

Batovska, D.I., Todorova, I.T., Parushev, S.P., Nedelcheva, D.V., Bankova, V.S., Popov, S.S., Ivanova, I.I., Batovski, S.A., 2009. Biomarkers for the prediction of the resistance and susceptibility of grapevine leaves to downy mildew. J. Plant Physiol. 166, 781–785. https://doi.org/10.1016/j.jplph.2008.08.008.

Becker, L., Poutaraud, A., Hamm, G., Muller, J.-F., Merdinoglu, D., Carré, V., Chaimbault, P., 2013. Metabolic study of grapevine leaves infected by downy mildew using negative ion electrospray – Fourier transform ion cyclotron resonance mass spectrometry. Anal. Chim. Acta 795, 44–51. https://doi.org/10.1016/j.aca.2013.07.068.

Berger, S., Papadopoulos, M., Schreiber, U., Kaiser, W., Roitsch, T., 2004. Complex regulation of gene expression, photosynthesis and sugar levels by pathogen infection in tomato. Physiol. Plantarum 122, 419–428. https://doi.org/10.1111/j.1399-3054.2004.00433.x.

Berger, S., Sinha, A.K., Roitsch, T., 2007. Plant physiology meets phytopathology: plant primary metabolism and plant–pathogen interactions. J. Exp. Bot. 58, 4019–4026. https://doi.org/10.1093/jxb/erm298.

Buonassisi, D., Colombo, M., Migliaro, D., Dolzani, C., Peressotti, E., Mizzotti, C., Velasco, R., Masiero, S., Perazzolli, M., Vezzulli, S., 2017. Breeding for grapevine downy mildew resistance: a review of "omics" approaches. Euphytica 213. https://doi.org/10.1007/s10681-017-1882-8.

Childs, R.E., Bardsley, W.G., 1975. The steady-state kinetics of peroxidase with 2,2'-azino-di-(3-ethyl-benzthiazoline-6-sulphonic acid) as chromogen. Biochem. J. 145, 93–103.

Chitarrini, G., Soini, E., Riccadonna, S., Franceschi, P., Zulini, L., Masuero, D., Vecchione, A., Stefanini, M., Di Gaspero, G., Mattivi, F., Vrhovsek, U., 2017. Identification of Biomarkers for Defense Response to *Plasmopara viticola* in a Resistant Grape Variety. Front. Plant Sci. 8. https://doi.org/10.3389/fpls.2017.01524.

Chong, J., Soufan, O., Li, C., Caraus, I., Li, S., Bourque, G., Wishart, D.S., Xia, J., 2018. MetaboAnalyst 4.0: towards more transparent and integrative metabolomics analysis. Nucleic Acids Res. 46, W486–W494. https://doi.org/10.1093/nar/gky310.

Dufourc, E.J., 2008. The role of phytosterols in plant adaptation to temperature. Plant Signal. Behav. 3, 133–134.

Fahy, E., Cotter, D., Sud, M., Subramaniam, S., 2011. Lipid classification, structures and tools. Biochim. Biophys. Acta BBA - Mol. Cell Biol. Lipids 1811, 637–647. https://doi.org/10.1016/j.bbalip.2011.06.009.

Figueiredo, A., Fortes, A., Ferreira, S., Sebastiana, M., Choi, Y., Sousa, L., Acioli-Santos, B., Pessoa, F., Verpoorte, R., Pais, M.S., 2008. Transcriptional and metabolic profiling of grape (*Vitisvinifera* L.) leaves unravel possible innate resistance against pathogenic fungi. J. Exp. Bot 59 (12), 3371–3381. https://doi.org/10.1093/jxb/ern187.

Figueiredo, A., Martins, J., Sebastiana, M., Guerreiro, A., Silva, A., Matos, A.R., Monteiro, F., Pais, M.S., Roepstorff, P., Coelho, A.V., 2017. Specific adjustments in grapevine leaf proteome discriminating resistant and susceptible grapevine genotypes to *Plasmopara viticola*. J. Proteomics 152, 48–57. https://doi.org/10.1016/j.jprot.2016.10.012.

Figueiredo, A., Monteiro, F., Fortes, A.M., Bonow-Rex, M., Zyprian, E., Sousa, L., Pais, M.S., 2012. Cultivar-specific kinetics of gene induction during downy mildew early infection in grapevine. Funct. Integr. Genom. 12, 379–386. https://doi.org/10.1007/s10142-012-0261-8.

Ford, D.A., 2010. Lipid oxidation by hypochlorous acid: chlorinated lipids in atherosclerosis and myocardial ischemia. Clin. Lipidol. 5, 835–852. https://doi.org/10.2217/clp.10.68.

Fung, R.W.M., Gonzalo, M., Fekete, C., Kovacs, L.G., He, Y., Marsh, E., McIntyre, L.M., Schachtman, D.P., Qiu, W., 2008. Powdery Mildew Induces Defense-Oriented Reprogramming of the Transcriptome in a Susceptible But Not in a Resistant Grapevine. Plant Physiol. 146, 236–249. https://doi.org/10.1104/pp.107.108712.

Gaspero, G.D., Cipriani, G., Adam-Blondon, A.-F., Testolin, R., 2007. Linkage maps of grapevine displaying the chromosomal locations of 420 microsatellite markers and 82 markers for R-gene candidates. Theor. Appl. Genet. 114, 1249–1263. https://doi.org/10.1007/s00122-007-0516-2.

Gebrie, S.A., 2016. Biotrophic Fungi Infection and Plant Defense Mechanism. J. Plant Pathol. Microbiol. 7, 1–6. https://doi.org/10.4172/2157-7471.1000378.
Gessler, C., Pertot, I., Perazzolli, M., 2011. Plasmopara viticola: a review of knowledge on downy mildew of grapevine and effective disease management. Phytopathol. Mediterr. 50, 3–44. https://doi.org/10.14601/Phytopathol_Mediterr-9360.
Gindro, K., Pezet, R., Viret, O., 2003. Histological study of the responses of two Vitis vinifera cultivars (resistant and susceptible) to Plasmopara viticola infections. Plant Physiol. Biochem. 41, 846–853. https://doi.org/10.1016/S0981-9428(03)00124-4.
Guerreiro, A., Figueiredo, J., Sousa Silva, M., Figueiredo, A., 2016. Linking jasmonic acid to grapevine resistance against the biotrophic oomycete Plasmopara viticola. Front. Plant Sci. https://doi.org/10.3389/fpls.2016.00565.
Guillier, C., Gamm, M., Lucchi, G., Truntzer, C., Pecqueur, D., Ducoroy, P., Adrian, M., Héloir, M.-C., 2015. Toward the Identification of Two Glycoproteins Involved in the Stomatal Deregulation of Downy Mildew–Infected Grapevine Leaves. Mol. Plant Microbe Interact. 28, 1227–1236. https://doi.org/10.1094/MPMI-05-15-0115-R.
Gunnaiah, R., Kushalappa, A.C., 2014. Metabolomics deciphers the host resistance mechanisms in wheat cultivar Sumai-3, against trichothecene producing and non-producing isolates of Fusarium graminearum. Plant Physiol. Biochem. PPB 83, 40–50. https://doi.org/10.1016/j.plaphy.2014.07.002.
Guy, C.L., Huber, J.L.A., Huber, S.C., 1992. Sucrose Phosphate Synthase and Sucrose Accumulation at Low Temperature. Plant Physiol. 100, 502–508. https://doi.org/10.1104/pp.100.1.502.
Hamiduzzaman, M.M., Jakab, G., Barnavon, L., Neuhaus, J.-M., Mauch-Mani, B., 2005. β-Aminobutyric Acid-Induced Resistance Against Downy Mildew in Grapevine Acts Through the Potentiation of Callose Formation and Jasmonic Acid Signaling. Mol. Plant Microbe Interact. 18, 819–829. https://doi.org/10.1094/MPMI-18-0819.
Hayes, M.A., Feechan, A., Dry, I.B., 2010. Involvement of abscisic acid in the coordinated regulation of a stress-inducible hexose transporter (VvHT5) and a cell wall invertase in grapevine in response to biotrophic fungal infection. Plant Physiol. 153, 211–221. https://doi.org/10.1104/pp.110.154765.
Hellemans, J., Mortier, G., De Paepe, A., Speleman, F., Vandesompele, J., 2007. qBase relative quantification framework and software for management and automated analysis of real-time quantitative PCR data. Genome Biol. 8, R19. https://doi.org/10.1186/gb-2007-8-2-r19.
Hodges, D.M., DeLong, J.M., Forney, C.F., Prange, R.K., 1999. Improving the thiobarbituric acid-reactive-substances assay for estimating lipid peroxidation in plant tissues containing anthocyanin and other interfering compounds. Planta 207, 604–611. https://doi.org/10.1007/s004250050524.
Hofmann, S.G., Sawyer, A.T., Witt, A.A., Oh, D., 2010. The Effect of Mindfulness-Based Therapy on Anxiety and Depression: A Meta-Analytic Review. J. Consult. Clin. Psychol. 78, 169–183. https://doi.org/10.1037/a0018555.
Horn, P.J., Chapman, K.D., 2014. Lipidomics in situ: Insights into plant lipid metabolism from high resolution spatial maps of metabolites. Prog. Lipid Res. 54, 32–52. https://doi.org/10.1016/j.plipres.2014.01.003.
Hou, Q., Ufer, G., Bartels, D., 2016. Lipid signalling in plant responses to abiotic stress. Plant Cell Environ. 39, 1029–1048. https://doi.org/10.1111/pce.12666.
Kamoun, S., Furzer, O., Jones, J.D.G., Judelson, H.S., Ali, G.S., Dalio, R.J.D., Roy, S.G., Schena, L., Zambounis, A., Panabières, F., Cahill, D., Ruocco, M., Figueiredo, A., Chen, X.-R., Hulvey, J., Stam, R., Lamour, K., Gijzen, M., Tyler, B.M., Grünwald, N.J., Mukhtar, M.S., Tomé, D.F.A., Tör, M., Van Den Ackerveken, G., McDowell, J., Daayf, F., Fry, W.E., Lindqvist-Kreuze, H., Meijer, H.J.G., Petre, B., Ristaino, J., Yoshida, K., Birch, P.R.J., Govers, F., 2015. The Top 10 oomycete pathogens in molecular plant pathology. Mol. Plant Pathol. 16, 413–434. https://doi.org/10.1111/mpp.12190.
Kanehisa, M., Sato, Y., Kawashima, M., Furumichi, M., Tanabe, M., 2016. KEGG as a reference resource for gene and protein annotation. Nucleic Acids Res. 44, D457–D462. https://doi.org/10.1093/nar/gkv1070.
Kortekamp, A., 2006. Expression analysis of defence-related genes in grapevine leaves after inoculation with a host and a non-host pathogen. Plant Physiol. Biochem. 44, 58–67. https://doi.org/10.1016/j.plaphy.2006.01.008.
Kortekamp, A., Welter, L., Vogt, S., Knoll, A., Schwander, F., Töpfer, R., Zyprian, E., 2008. Identification, isolation and characterization of a CC-NBS-LRR candidate disease resistance gene family in grapevine. Mol. Breed 22, 421–432. https://doi.org/10.1007/s11032-008-9186-2.
La Camera, S., Gouzerh, G., Dhondt, S., Hoffmann, L., Fritig, B., Legrand, M., Heitz, T., 2004. Metabolic reprogramming in plant innate immunity: the contributions of phenylpropanoid and oxylipin pathways. Immunol. Rev. 198, 267–284.
Laloi, M., Perret, A.-M., Chatre, L., Melser, S., Cantrel, C., Vaultier, M.-N., Zachowski, A., Bathany, K., Schmitter, J.-M., Vallet, M., Lessire, R., Hartmann, M.-A., Moreau, P., 2007. Insights into the Role of Specific Lipids in the Formation and Delivery of Lipid Microdomains to the Plasma Membrane of Plant Cells. Plant Physiol. 143, 461–472. https://doi.org/10.1104/pp.106.091496.
Latouche, G., Bellow, S., Poutaraud, A., Meyer, S., Cerovic, Z.G., 2013. Influence of constitutive phenolic compounds on the response of grapevine (*Vitis vinifera* L.) leaves to infection by Plasmopara viticola. Planta 237, 351–361. https://doi.org/10.1007/s00425-012-1776-x.
Legay, G., Marouf, E., Berger, D., Neuhaus, J.-M., Mauch-Mani, B., Slaughter, A., 2011. Identification of genes expressed during the compatible interaction of grapevine with *Plasmopara viticola* through suppression subtractive hybridization (SSH). Eur. J. Plant Pathol. 129, 281–301. https://doi.org/10.1007/s10658-010-9676-z.
Lichtenthaler, H.K., 1987. Chlorophylls and carotenoids: Pigments of photosynthetic biomembranes. Methods Enzymol. Plant Cell Membranes 148, 350–382. https://doi.org/10.1016/0076-6879(87)48036-1.
Lim, G.-H., Singhal, R., Kachroo, A., Kachroo, P., 2017. Fatty Acid– and Lipid-Mediated Signaling in Plant Defense. Annu. Rev. Phytopathol. 55, 505–536. https://doi.org/10.1146/annurev-phyto-080516-035406.
Liu, R., Wang, L., Zhu, J., Chen, T., Wang, Y., Xu, Y., 2015. Histological responses to downy mildew in resistant and susceptible grapevines. Protoplasma 252, 259–270. https://doi.org/10.1007/s00709-014-0677-1.
Ma, H., Xiang, G., Li, Z., Wang, Y., Dou, M., Su, L., Yin, X., Liu, R., Wang, Y., Xu, Y., 2018. Grapevine VpPR10.1 functions in resistance to *Plasmopara viticola* through triggering a cell death-like defence response by interacting with VpVDAC3. Plant Biotechnol. J. 16, 1488–1501. https://doi.org/10.1111/pbi.12891.
Madden, L.V., Ellis, M.A., Lalancette, N., Hughes, G., Wilson, L.L., 2000. Evaluation of a Disease Warning System for Downy Mildew of Grapes. Plant Dis. 84, 549–554. https://doi.org/10.1094/PDIS.2000.84.5.549.
Madi, L., Wang, X., Kobiler, I., Lichter, A., Prusky, D., 2003. Stress on avocado fruits regulates Δ9-stearoyl ACP desaturase expression, fatty acid composition, antifungal diene level and resistance to Colletotrichum gloeosporioides attack. Physiol. Mol. Plant Pathol. 62, 277–283. https://doi.org/10.1016/S0885-5765(03)00076-6.
Maia, M., Monteiro, F., Sebastiana, M., Marques, A.P., Ferreira, A.E.N., Freire, A.P., Cordeiro, C., Figueiredo, A., Sousa Silva, M., 2016. Metabolite extraction for high-throughput FTICR-MS-based metabolomics of grapevine leaves. EuPA Open Proteomics 12, 4–9. https://doi.org/10.1016/j.euprot.2016.03.002.
Mandal, S., Das, R.K., Mishra, S., 2011. Differential occurrence of oxidative burst and antioxidative mechanism in compatible and incompatible interactions of Solanum lycopersicum and Ralstonia solanacearum. Plant Physiol. Biochem. 49, 117–123. https://doi.org/10.1016/j.plaphy.2010.10.006.
McGovern, P.E., Glusker, D.L., Exner, L.J., Voigt, M.M., 1996. Neolithic resinated wine. Nature 381, 480–481. https://doi.org/10.1038/381480a0.
Mierziak, J., Kostyn, K., Kulma, A., 2014. Flavonoids as Important Molecules of Plant Interactions with the Environment. Molecules 19, 16240–16265. https://doi.org/10.3390/molecules191016240.
Milli, A., Cecconi, D., Bortesi, L., Persi, A., Rinalducci, S., Zamboni, A., Zoccatelli, G., Lovato, A., Zolla, L., Polverari, A., 2012. Proteomic analysis of the compatible interaction between *Vitis vinifera* and *Plasmopara viticola*. J. Proteomics 75, 1284–1302. https://doi.org/10.1016/j.jprot.2011.11.006.
Monteiro, F., Sebastiana, M., Pais, M.S., Figueiredo, A., 2013. Reference Gene Selection and Validation for the Early Responses to Downy Mildew Infection in Susceptible and Resistant Vitis vinifera Cultivars. PLoS One 8, e72998. https://doi.org/10.1371/journal.pone.0072998.
Moriondo, M., Orlandini, S., Giuntoli, A., Bindi, M., 2005. The Effect of Downy and Powdery Mildew on Grapevine (Vitis vinifera L.) Leaf Gas Exchange. J. Phytopathol. 153, 350–357. https://doi.org/10.1111/j.1439-0434.2005.00984.x.
Nakamura, Y., Mochamad Afendi, F., Kawsar Parvin, A., Ono, N., Tanaka, K., Hirai Morita, A., Sato, T., Sugiura, T., Altaf-Ul-Amin, M., Kanaya, S., 2014. KNApSAcK Metabolite Activity Database for Retrieving the Relationships Between Metabolites and Biological Activities. Plant Cell Physiol. 55 e7–e7. https://doi.org/10.1093/pcp/pct176.
Nishizawa, A., Yabuta, Y., Shigeoka, S., 2008. Galactinol and raffinose constitute a novel function to protect plants from oxidative damage. Plant Physiol. 147, 1251–1263. https://doi.org/10.1104/pp.108.122465.
Nishizawa-Yokoi, A., Yabuta, Y., Shigeoka, S., 2008. The contribution of carbohydrates including raffinose family oligosaccharides and sugar alcohols to protection of plant cells from oxidative damage. Plant Signal. Behav. 3, 1016–1018.
O'Connell, R.J., Panstruga, R., 2006. Tête à tête inside a plant cell: establishing compatibility between plants and biotrophic fungi and oomycetes. New Phytol. 171, 699–718. https://doi.org/10.1111/j.1469-8137.2006.01829.x.
Ogata, H., Goto, S., Sato, K., Fujibuchi, W., Bono, H., Kanehisa, M., 1999. KEGG: Kyoto Encyclopedia of Genes and Genomes. Nucleic Acids Res. 27, 29–34. https://doi.org/10.1093/nar/27.1.29.
Organization of Vine and Wine, 2017. 2017 OIV Statistical Report on World Vitiviniculture.
Patel, T.K., Williamson, J.D., 2016. Mannitol in Plants, Fungi, and Plant-Fungal Interactions. Trends Plant Sci. 21, 486–497. https://doi.org/10.1016/j.tplants.2016.01.006.
Perazzolli, M., Moretto, M., Fontana, P., Ferrarini, A., Velasco, R., Moser, C., Delledonne, M., Pertot, I., 2012. Downy mildew resistance induced by Trichoderma harzianum T39 in susceptible grapevines partially mimics transcriptional changes of resistant genotypes. BMC Genomics 13, 660. https://doi.org/10.1186/1471-2164-13-660.
Perazzolli, M., Palmieri, M.C., Matafora, V., Bachi, A., Pertot, I., 2016. Phosphoproteomic analysis of induced resistance reveals activation of signal transduction processes by beneficial and pathogenic interaction in grapevine. J. Plant Physiol. 195, 59–72. https://doi.org/10.1016/j.jplph.2016.03.007.
Polesani, M., Bortesi, L., Ferrarini, A., Zamboni, A., Fasoli, M., Zadra, C., Lovato, A., Pezzotti, M., Delledonne, M., Polverari, A., 2010. General and species-specific transcriptional responses to downy mildew infection in a susceptible (Vitis vinifera) and a resistant (V. riparia) grapevine species. BMC Genomics 11, 117. https://doi.org/10.1186/1471-2164-11-117.
Polesani, M., Desario, F., Ferrarini, A., Zamboni, A., Pezzotti, M., Kortekamp, A., Polverari, A., 2008. cDNA-AFLP analysis of plant and pathogen genes expressed in grapevine infected with *Plasmopara viticola*. BMC Genomics 9, 142. https://doi.org/10.1186/1471-2164-9-142.
Rossin, G., Villalta, D., Martelli, P., Cecconi, D., Polverari, A., Zoccatelli, G., 2015. Grapevine Downy Mildew Plasmopara viticola Infection Elicits the Expression of Allergenic Pathogenesis-Related Proteins. Int. Arch. Allergy Immunol. 168, 90–95. https://doi.org/10.1159/000441792.
Schneider, T., Keller, F., 2009. Raffinose in chloroplasts is synthesized in the cytosol and transported across the chloroplast envelope. Plant Cell Physiol. 50, 2174–2182. https://doi.org/10.1093/pcp/pcp151.
Sebastiana, M., Martins, J., Figueiredo, A., Monteiro, F., Sardans, J., Peñuelas, J., Silva, A., Roepstorff, P., Pais, M.S., Coelho, A.V., 2017. Oak protein profile alterations upon root colonization by an ectomycorrhizal fungus. Mycorrhiza 27, 109–128. https://

doi.org/10.1007/s00572-016-0734-z.
Shah, J., 2005. Lipids, lipases, and lipid-modifying enzymes in plant disease resistance. Annu. Rev. Phytopathol. 43, 229–260. https://doi.org/10.1146/annurev.phyto.43.040204.135951.
Singh, R., Dangol, S., Chen, Y., Choi, J., Cho, Y.-S., Lee, J.-E., Choi, M.-O., Jwa, N.-S., 2016. Magnaporthe oryzae Effector AVR-Pii Helps to Establish Compatibility by Inhibition of the Rice NADP-Malic Enzyme Resulting in Disruption of Oxidative Burst and Host Innate Immunity. Mol. Cell. 39, 426–438. https://doi.org/10.14348/molcells.2016.0094.
Su, H., Jiao, Y.-T., Wang, F.-F., Liu, Y.-E., Niu, W.-L., Liu, G.-T., Xu, Y., 2018. Overexpression of VpPR10.1 by an efficient transformation method enhances downy mildew resistance in V. vinifera. Plant Cell Rep. 37, 819–832. https://doi.org/10.1007/s00299-018-2271-z.
Sud, M., Fahy, E., Cotter, D., Brown, A., Dennis, E.A., Glass, C.K., Merrill, A.H., Murphy, R.C., Raetz, C.R.H., Russell, D.W., Subramaniam, S., 2007. LMSD: LIPID MAPS structure database. Nucleic Acids Res. 35, D527–D532. https://doi.org/10.1093/nar/gkl838.
Suhre, K., Schmitt-Kopplin, P., 2008. MassTRIX: mass translator into pathways. Nucleic Acids Res. 36, W481–W484. https://doi.org/10.1093/nar/gkn194.
Supian, S., Saidi, N.B., Wee, C.-Y., Abdullah, M.P., 2017. Antioxidant-mediated response of a susceptible papaya cultivar to a compatible strain of Erwinia mallotivora. Physiol. Mol. Plant Pathol. 98, 37–45. https://doi.org/10.1016/j.pmpp.2017.02.005.
Swarbrick, P.J., Schulze-Lefert, P., Scholes, J.D., 2006. Metabolic consequences of susceptibility and resistance (race-specific and broad-spectrum) in barley leaves challenged with powdery mildew. Plant Cell Environ. 29, 1061–1076. https://doi.org/10.1111/j.1365-3040.2005.01472.x.
Torres, M.A., Jones, J.D.G., Dangl, J.L., 2006. Reactive Oxygen Species Signaling in Response to Pathogens. Plant Physiol. 141, 373–378. https://doi.org/10.1104/pp.106.079467.
Unger, S., Büche, C., Boso, S., Kassemeyer, H.-H., 2007. The Course of Colonization of Two Different *Vitis* Genotypes by *Plasmopara viticola* Indicates Compatible and Incompatible Host-Pathogen Interactions. Phytopathology 97, 780–786. https://doi.org/10.1094/PHYTO-97-7-0780.
Vandesompele, J., De Preter, K., Pattyn, F., Poppe, B., Van Roy, N., De Paepe, A., Speleman, F., 2002. Accurate normalization of real-time quantitative RT-PCR data by geometric averaging of multiple internal control genes. Genome Biol. 3 research0034.1-research0034.11.
Vannozzi, A., Dry, I.B., Fasoli, M., Zenoni, S., Lucchin, M., 2012. Genome-wide analysis of the grapevine stilbene synthase multigenic family: genomic organization and expression profiles upon biotic and abiotic stresses. BMC Plant Biol. 12, 130. https://doi.org/10.1186/1471-2229-12-130.
Walley, J.W., Kliebenstein, D.J., Bostock, R.M., Dehesh, K., 2013. Fatty acids and early detection of pathogens. Curr. Opin. Plant Biol. 16, 520–526. https://doi.org/10.1016/j.pbi.2013.06.011.
Yi, X., Maeda, N., 2005. Endogenous production of lipoic acid is essential for mouse development. Mol. Cell Biol. 25, 8387–8392. https://doi.org/10.1128/MCB.25.18.8387-8392.2005.
Yin, X., Liu, R.-Q., Su, H., Su, L., Guo, Y.-R., Wang, Z.-J., Du, W., Li, M.-J., Zhang, X., Wang, Y.-J., Liu, G.-T., Xu, Y., 2017. Pathogen development and host responses to Plasmopara viticola in resistant and susceptible grapevines: an ultrastructural study. Hortic. Res. 4, 17033. https://doi.org/10.1038/hortres.2017.33.
Zauber, H., Burgos, A., Garapati, P., Schulze, W.X., 2014. Plasma membrane lipid-protein interactions affect signaling processes in sterol-biosynthesis mutants in Arabidopsis thaliana. Front. Plant Sci. 5, 78. https://doi.org/10.3389/fpls.2014.00078.